

1 Integration of dendrochronological and palaeoecological disturbance
2 reconstructions in temperate mountain forests

3

4 Niina Kuosmanen^a, Vojtěch Čada^a, Karen Halsall^b, Richard C. Chiverrell^b, Nick B. Schafstall^a, Petr
5 Kuneš^c, John F. Boyle^b, Milos Knížek^d, Peter G. Appleby^e, Miroslav Svoboda^a, Jennifer L. Clear^{a,f}

6

7 ^aDepartment of Forest Ecology, Faculty of Forestry and Wood Sciences, Czech University of Life
8 Sciences Prague, Czech Republic

9 ^bSchool of Environmental Sciences, University of Liverpool, Liverpool, UK

10 ^cDepartment of Botany, Faculty of Science, Charles University, Prague, Czech Republic

11 ^dDepartment of Forest Protection Service, Forestry and Game Management Research Institute,
12 Jíloviště - Strnady, Czech Republic

13 ^eEnvironmental Radioactivity Research Centre, University of Liverpool, Liverpool, UK

14 ^fDepartment of Geography and Environmental Science, Liverpool Hope University, Liverpool, UK

15

16 cada@fld.czu.cz, karen.halsall@gmail.com, r.c.chiverrell@liverpool.ac.uk, nick.schafstall@gmail.com,

17 petr.kunes@natur.cuni.cz, jfb@liverpool.ac.uk, knizek@vulhm.cz, svobodam@fld.czu.cz,

18 clearj@hope.ac.uk

19

20 **Corresponding author:**

21 Kuosmanen Niina, niina.kuosmanen@helsinki.fi

22 Department of Forest Ecology, Faculty of Forestry and Wood Sciences,

23 Czech University of Life Sciences Prague

24 Kamýcká 129, 165 00 Praha 6 – Suchbát, Czech Republic

25

26

27 **Highlights**

- 28 - Integration of dendrochronological and palaeoecological disturbance reconstructions.
29 - Increase in disturbances in temperate mountain spruce forests from 1600s.
30 - The concurrent occurrence of disturbance agents create a complex disturbance regime.
31 - Management and conservation strategies should consider the multiple disturbance agents.

32

33 **Abstract**

34 Disentangling the long-term changes in forest disturbance dynamics provides a basis for predicting
35 the forest responses to changing environmental conditions. The combination of multidisciplinary
36 records can offer more robust reconstructions of past forest disturbance dynamics. Here we link
37 disturbance histories of the central European mountain spruce forest obtained from
38 dendrochronological and palaeoecological records (fossil pollen, sedimentary charcoal, bark beetle
39 remains and geochemistry) using a small glacial lake and the surrounding forest in the Šumava
40 National Park (Czech Republic). Dendrochronological reconstructions of disturbance were created for
41 300-year-long records from 6 study plots with a minimum of 35 trees analyzed for the abrupt growth
42 increases (releases) and rapid early growth rates, both indicative of disturbance events. High-
43 resolution analysis of lake sediments were used to reconstruct 800-year long changes in forest
44 composition and landscape openness (fossil pollen), past fire events (micro- and macroscopic
45 charcoal), bark beetle occurrence (fossil bark beetle remains), and erosion episodes (geochemical
46 signals in the sediment) potentially resulting from disturbance events.

47

48 Tree-ring data indicate that disturbances occurred regularly through the last three centuries and
49 identify a most intensive period of disturbances between 1780 and 1830 CE. Geochemical erosion
50 markers (e.g. K, Zr, % inorganic) show greater flux of catchment sediment and soils in the periods
51 1250–1400 and 1450–1500 CE, before a substantial shift to a more erosive regime 1600–1850 and
52 1900 CE onwards. Pollen records demonstrate relatively small changes in forest composition during

53 last 800 years until the beginning of the 20th century, when there was decrease in *Picea*. Fossil bark
54 beetle remains indicate continuous presence of bark beetles from 1620s to 1800s, and charcoal
55 records suggest that more frequent fires occurred during the 18th century. Each of the
56 dendrochronological, palaeoecological and sedimentological records provide a unique perspective on
57 forest disturbance dynamics, and combined offer a more robust and complete record of disturbance
58 history. We demonstrate that sedimentary proxies originating from the lake catchment mirror the
59 forest disturbance dynamics recorded in the tree-rings. However, the multidisciplinary records likely
60 record forest disturbances at different spatial and temporal scales revealing different disturbances
61 characteristics. Integrating these multidisciplinary datasets demonstrates a promising way to obtain
62 more complete understanding of long-term disturbance dynamics. However, integrating datasets
63 with variable spatial and temporal influence remains challenging. Our results indicated that multiple
64 disturbance factors, such as windstorms, bark beetle outbreaks and fires, may occur simultaneously
65 creating a complex disturbance regime in mountain forests, which should be considered in forest
66 management and conservation strategies.

67

68 Keywords: Disturbance, forest dynamics, bark beetles, fire, pollen, geochemistry, tree-rings, *Picea*
69 *abies*

70

71 **1. Introduction**

72 Natural disturbances such as windthrows, insect outbreaks, droughts and fires maintain the high
73 diversity and structural characteristics of natural temperate forest ecosystems (Kulakowski et al.,
74 2017). In recent years, natural disturbances have intensified and the changing climate, together with
75 increasing anthropogenic influence, have put temperate mountain forests under increasing pressure
76 that may affect the resilience of these forests (Reyer et al., 2015; Thom et al., 2017). In central
77 European temperate mountain forests, insect outbreaks and windthrow events have caused large
78 disturbances during the last few decades (e.g. Schelhaas et al., 2003; Čada et al., 2013, 2016a;

79 HOLEKSA ET AL., 2017). Windstorms and insect outbreaks are considered as the main disturbance
80 agents in these mountain ecosystems. However, there is an increasing number of studies
81 demonstrating the importance of fire as a disturbance agent in temperate forest ecosystems (e.g.
82 NIKLASSON ET AL., 2010; FEURDEAN ET AL., 2017; BOBEK ET AL., 2018; CARTER ET AL., 2018) and predictions of
83 increasing climate extremes, such as droughts, may increase the future risk of fires in central
84 European ecosystems (IPCC). As it is uncertain how forest ecosystems will respond to the future
85 changes, knowledge of long-term changes of natural and human-induced disturbances, and
86 understanding the processes behind them is crucial to apply the best management practices to
87 maintain the ecological diversity and ecosystem services.

88
89 Dendrochronology has been widely used to reconstruct stand-scale disturbance dynamics and their
90 impact on forest ecosystems. These disturbance reconstructions from tree-rings can extend a few
91 hundred years back in time and provide valuable information about disturbance frequency and
92 severity (e.g. SVOBODA ET AL., 2013; ČADA ET AL., 2016a; HOLEKSA ET AL., 2017; JANDA ET AL., 2017).
93 However, it is problematic to assess the long-term changes in disturbance history based on
94 dendrochronological records alone, because these records usually span just one tree generation. It is
95 also impossible to identify the disturbance agent, because prevailing agents such as windstorms, bark
96 beetle outbreaks, and logging are not recorded in tree-rings by any specific feature. Palaeoecological
97 data, such as pollen, macrofossils, and charcoal, derived from sedimentary archives provide
98 information of past disturbance history over millennial scale and can provide means to assess the
99 possible disturbance agents in long-term perspective. Where dendrochronological data are accurate at
100 the spatial (single tree) and temporal (annual) scale, this accuracy is limited to km's and decades in
101 palaeoecological records, respectively. In addition to dendrochronological and palaeoecological
102 records, physical properties of lake sediments, measured using the sediment geochemistry and grain
103 size, reflect erosion events (e.g. floods) and change in the baseline erosion regime of the catchment
104 (Davies et al., 2015). Physical properties thereby provide means for identifying potential landscape

105 responses to forest disturbances. These multidisciplinary approaches used to reconstruct
106 disturbances reveal different spatial and temporal aspects of disturbance regimes, and highlight the
107 effects that disturbances can have on forest ecosystems. This highlights the importance of
108 integrating multidisciplinary records to enable us to understand the complex processes behind the
109 mountain forest dynamics. The integration of dendrochronological, palaeoecological and
110 sedimentological records in disturbance reconstructions provide a more robust and complete record
111 of disturbance history, and are essential to identify the impact of disturbances on forest ecosystems
112 with changing climate dynamics.

113

114 There have been previous studies including both dendrochronological and palaeoecological methods
115 to reconstruct for example past climate (e.g. Edwards and Dunwiddie 1985; Helama et al. 2012),
116 natural and anthropogenic environmental change (e.g. McLachan et al. 2000) and past fire dynamics
117 from fire scars (e.g. Niklasson et al., 2002; Drobyshev et al., 2004; Higuera et al., 2005; Stivrins et al.,
118 2019). Here we link, for the first time to our knowledge, dendrochronological (300-years long)
119 disturbance reconstruction based on changes in tree-ring width with multiproxy sedimentological
120 and palaeoecological (800-years long) datasets from a central European mountain spruce forest, in
121 which windthrows and bark beetle outbreaks are expected to be the prevailing disturbance agents.
122 Precise dendrochronological disturbance reconstruction based on trees' growth rate changes is
123 coupled with; 1) high-resolution fossil pollen records to reconstruct the changes in forests
124 composition and landscape openness, 2) sedimentary charcoal to reveal the past fire events, 3) fossil
125 bark beetle remains to identify insect outbreaks, and 4) variations in sediment geochemistry and
126 grains size to detect changes in the catchment erosion regime associated with disturbance events in
127 the lake catchment. The main objectives are to i) produce a long-term (800 years) disturbance history
128 in the mountain spruce forest, ii) to assess the possible disturbance agents and the impacts in the
129 lake catchment and iii) to evaluate the integration of dendrochronological, palaeoecological and
130 sedimentological data in providing a multidisciplinary reconstruction of forest disturbance history.

131

132 **2. Methods**

133 2.1 Study area

134 The study area is located in the temperate vegetation zone in Bohemian Forest, Šumava National
135 Park (NP), Czech Republic, central Europe (Fig. 1). Bedrock of the lake catchment belongs to the
136 crystalline complex of the Bohemian massive and consists of gneisses (Cháb et al., 2007). Soils are
137 shallow and poor, dominated by podsoles and stony soils (Kozák, 2010). Climate is cold with mean
138 annual temperature of 4 °C, and a mean annual precipitation of 1200 mm (Tolasz et al., 2007). The
139 mountain glacier in the area was deglaciated ~14,000 cal yr BP (Mentlík et al., 2010). The study site,
140 Laka is a shallow (maximum depth 4 m) mesotrophic lake located at 1096 m.a.s.l. being at the highest
141 elevation of the eight glacial lakes formed in the glacial cirques in the Bohemian Forest. It is also the
142 smallest with surface area of circa 2.8 ha, a catchment area of 1,35 km² and catchment:lake area
143 ratio at 48:1, which is conducive for recording catchment processes.

144

145 [Figure 1.]

146

147 The present vegetation in the Laka catchment is composed of the nearly monospecific Norway
148 spruce (*Picea abies*) forests, with minor components of rowan (*Sorbus aucuparia*), Sycamore maple
149 (*Acer pseudoplatanus*), fir (*Abies alba*), and beech (*Fagus sylvatica*) (Neuhäuslová and Moravec,
150 1998). The vegetation community is mostly comprised of grass species *Calamagrostio villosae-*
151 *Piceetum*; with patches dominated by *Calamagrostis villosa* (Chaix), *Deschampsia flexuosa*, and
152 blueberry (*Vaccinium myrtillus*) growing on more stony soils (Neuhäuslová and Moravec, 1998).

153

154 The Mountain regions in Šumava NP have remained in relatively natural conditions until fairly
155 recently. Intensive colonization of the foothills and logging of the Bohemian Forest linked to the glass
156 and metallurgy industries occurred during the 14th century. However, the higher parts of the

157 Bohemian forests were not colonized until the 18th century onwards (Kozáková et al., 2015). Old
158 growth forest with minimal human disturbance during last centuries (Čada et al., 2016a)
159 characterizes the mountain spruce forests surrounding the lake catchment, which provides valuable
160 opportunity to assess the natural processes behind the disturbance history.

161

162 2.2 Dendrochronological analyses

163 Six plots used for the dendrochronological analysis is located circa 0.2–1.6 km from the lake (Fig. 1).
164 Four of these plots were already published in landscape level study of Čada et al. (2016a) and two
165 plots were additionally sampled for this study using the same method. The plot size was 1000 m² to
166 obtain increment cores from at least 35 trees within the plot. The ring width measurement and cross
167 dating of increment cores were conducted using standard techniques. In accordance to traditional
168 dendrochronological approach, individual tree-ring series were analyzed for two ring-width patterns
169 that indicate past disturbance events: abrupt and sustained growth increases (releases from
170 suppression) and rapid early growth rates (Lorimer and Frelich, 1989). In order to classify annual
171 tree-ring growth as a release, the absolute growth increase between subsequent 10-year means had
172 to exceed 0.55 mm. In case there were multiple subsequent years exceeding the 0.55 mm release
173 threshold, the maximum growth year within a 20-year interval (± 10 years) was identified as a release
174 year. The average ring width of 6th–15th ring had to exceed 1.0 mm to classify the first year of the
175 series as a year of rapid early growth rate (Čada et al., 2016a). The threshold values specific for
176 Norway spruce were obtained from the literature and have been verified during our previous studies
177 using extensive tree-ring data and our experience with growth variation of the species (see; Čada et
178 al. 2016a). The stand-level disturbance chronology was based on the number of trees that indicated a
179 disturbance event at each decade relative to the number of trees available within a given decade.
180 The beginning of the chronology was set to 1720s, when the number of available trees and plots was
181 5 and 3, respectively. The number of samples and the robustness of dendrochronological disturbance
182 estimations increased dramatically after 1800s (87 and 6 available trees and plots, respectively).

183

184 2.3 Sediment sampling

185 A 1.5 m sediment profile (Laka 15-1) was collected from 1.6 m depth of water and sampled from a
186 floating platform using a Russian-style (1.5 x 0.075 m) corer. The sediment-water interface was
187 collected using a gravity corer (Laka 15-1GC) (Boyle, 1995). The cores were taken to the laboratory in
188 the University of Liverpool for wet sediment geochemical analysis (Olympus Delta XRF) and high-
189 resolution (15 µm) photography under uniform lighting with a Linescan Camera on a Geotek Multi-
190 sensor Core logger and subsampling. Sediment core were stored at + 4 °C for further analysis.
191 Subsamples were taken at 1 cm intervals to analyse fossil pollen and non-pollen-palynomorphs,
192 micro- and macroscopic charcoal, fossil beetles, particle size, near-infrared spectrometry and dry
193 mass specific geochemistry using an energy dispersive X-ray Florescence (ED-XRF) analyser.

194

195 2.4 Sediment chronology

196 Independent age control for the top 10 cm of the sediment profile at Laka was determined using
197 records of the fallout radionuclides Pb-210, Cs-137 and Am-241 (Appleby and Oldfield, 1978; Appleby
198 et al., 1991) (Table 1). Measurements of these radionuclides were carried out by direct gamma
199 spectrometry using Ortec HPGe GWL series well-type coaxial low background intrinsic germanium
200 detectors (Appleby et al., 1986) at the Environmental Radioactivity Research Centre in Liverpool, UK
201 (See more detailed description from APPENDIX A.1).

202

203 The stratigraphy of the long-core was secured by 10 AMS C-14 dates (Table 1) targeting hand-picked
204 terrestrial-sourced plant macrofossils (e.g. *Picea abies* needles) measured at the Poznań Radiocarbon
205 Laboratory, Poland. All the geochronological data (Table 1) including the sediment surface (2015)
206 were integrated within a Bayesian age-depth modelling routine 'BACON' (Blaauw and Christen, 2011)
207 using a Student-t distribution that considers scatter in the ¹⁴C measurements and allows for statistical
208 outliers. The Bayesian analysis (Christen and Perez, 2009) partitioned the core into 36 sections (0.05

209 m thick) estimating the accumulation rate for each segment using a Markov Chain Monte Carlo
 210 (MCMC) approach. The modelling was constrained by a prior model of sediment accumulation rate (a
 211 gamma distribution with mean 5-year cm⁻¹ and shape 1.5) and its variability (memory, a beta
 212 distribution with mean 0.32 and shape 18). All ¹⁴C ages were calibrated and modelled in 'BACON'
 213 using the IntCal13 curve (Reimer et al., 2013) (Fig. 2).

214

215 Table 1. Radiocarbon results for the long-core Laka-15 and lead 210 dating results for core LAK 15-
 216 1GC

217	Depth	Laboratory	¹⁴ C Age ±	Assigned ²¹⁰ Pb	Assigned age	Material
218	(cm)	ID		(Year CE)	(cal yr BP)	
219	163	Pb210_1		2015 ± 0	-65	
220	164.5	Pb210_2		2009 ± 1	-59	
221	165.5	Pb210_3		1996 ± 2	-48	
222	166.5	Pb210_4		1981 ± 3	-31	
223	167.5	Pb210_5		1965 ± 4	-15	
224	168.5	Pb210_6		1948 ± 5	2	
225	169.5	Pb210_7		1933 ± 6	17	
226	170.5	Pb210_8		1925 ± 7	25	
227	171.5	Pb210_9		1925 ± 7	25	
228	172.5	Pb210_10		1915	35	
229	173.5	Pb210_11		1899	51	
230	193.5	Poz-81584	130 ± 30			Plant material
231	207.5	Poz-94514	340 ± 30			Plant material
232	220.5	Poz-84784	195 ± 30			Plant material
233	244.5	Poz-84785	150 ± 30			Plant material
234	274.5	Poz-85123	310 ± 30			Plant material
235	305.5	Poz-85124	630 ± 30			Plant material
236	325.5	Poz-94517	880 ± 30			Plant material

237

238

239 [Figure 2.]

240

241 2.5 Sedimentary analyses

242 *2.5.1 Physical properties and geochemistry*

243 The long and gravity cores were subsampled at 1 cm intervals, freeze dried for 48 – 60 hours
244 collecting water content data (%). Major and trace element concentrations were determined using a
245 Bruker S2 Ranger ED-XRF for the gravity core and Spectro XEPOS 3 ED-XRF for the long core. For both
246 ED-XRF, the samples were hand pressed and measured under a He atmosphere under combined Pd
247 and Co excitation radiation and using a high resolution, low spectral interference silicon drift
248 detector. Daily standardisation procedures provide a system check on both ED-XRF and they have
249 comparable accuracies verified using 18 certified reference materials (Boyle et al., 2015). Particle size
250 distributions (PSD) were measured for all samples across the range 0.375–2000 μm using a Coulter LS
251 13 320 Single-Wavelength Laser Diffraction Particle Size Analyser. Hot H_2O_2 pretreatment removed
252 organic matter from the PSD samples, with samples dispersed $\text{Na}_6\text{O}_{18}\text{P}_6$, sonicated and run under
253 sonicating measurement conditions. Results are the average of three repeats following elimination of
254 outliers. The Coulter LS320 undergoes regular calibration checks using samples with known size
255 distributions and particle size frequency statistics were calculated using standard geometric formulae
256 using the GRADISTAT 8.0 software (Blott and Pye, 2001).

257
258 Near Infrared Spectrometry (NIRS) by diffuse reflectance were measured for all sediment samples
259 using a Bruker MPA Fourier-Transform NIRS using an integrating sphere. All samples were
260 homogenised by grinding and were lightly hand pressed, with the NIR spectra produced from 64
261 scans at an 8 cm^{-1} interval across the range 3595–12500 cm^{-1} . We used multiple regression of the NIR
262 spectra for a selection known composition end-member materials (EMS-MR, Russell et al., 2019) to
263 interpret the unknown composition lake sediment samples from Lake Laka. The EMS-RC provides
264 simultaneous quantification of major sediment components; here these were end member spectra
265 for local bedrock, biogenic silica (diatoms) and organic matter (see Russell et al. 2019). The end
266 members were minerogenic late glacial muds from nearby Prášílské lake, which we regard as
267 representative of the catchment bedrock. A marine diatom sample treated with H_2O_2 to remove any

268 organic material to reflect the proportion of biogenic silica. The organic component of the lake
269 sediment were rationalised to an ombrotrophic peat sample including less decomposed plant
270 remains and humic compounds. The fitting of these end member materials included sensitivity
271 analysis using other end member selections for all three components across a wider library of
272 materials to obtain the overall best fitting performance, defined by high R^2 of the sample multiple
273 regressions (> 0.85).

274

275 The catchment-lake area ratio (48:1) for Laka is conducive to efficient flux of detrital materials from
276 catchment to the lake, and so the down core patterns of major geochemical elements are likely to
277 reflect changes in the erosion regime. Geochemical ratios for Si:Al and Zr:Rb provide information on
278 indications of biogenic silica and the presence of coarser grain sizes, respectively (Davies et al., 2015).
279 Changes sediment sources, availability and the energy in the catchment most likely guided changing
280 in properties like the mean grain size, the coarsest grains (e.g. 90th percentile) and degree of sorting.
281 The NIR spectra provide parallel reconstructions of the proportions mineral, biogenic silica (diatom)
282 and organic matter in the sediments. Principal components analysis (PCA) was used to explore the
283 relationships between geochemical, grain size and NIRS down-core patterns. A stratigraphically
284 constrained cluster analysis for all these parameters, after standardisation to \pm one standard
285 deviation unit length, produced dendrograms that identify the major changes in the stratigraphy.

286

287 *2.5.2 Pollen and non-pollen palynomorph analysis*

288 Subsamples of 0.5 cm³ were extracted in 1 cm resolution and processed standard procedures of KOH-
289 , acetolysis- and HF-treatment (Fægri et al. 1989). In order to calculate microfossil concentrations
290 (grains cm⁻³) and accumulation rates (PAR; grains cm⁻² yr) *Lycopodium* marker spores were added
291 into the subsamples (Stockmarr, 1972) prior-to the sample preparation. The samples were mounted
292 in glycerine and a minimum of 500 terrestrial pollen grains were identified using a 400x
293 magnification. Pollen identification is based on Beug (2004), Moore et al. (1991), and a reference

294 collection at Charles University in Prague. Results are presented as a proportion of each pollen taxon
295 from the total sum of terrestrial taxa. The pollen ratio between the sum of arboreal pollen (AP) taxa
296 and the sum of non-arboreal pollen (NAP) taxa indicating more open landscape were used to detect
297 opening of forest canopy related to disturbance events. The summed percentage of Cerealia-type,
298 *Secale cereale*, *Centaurea cyanus*-type, *Fagopyrum*, *Plantago* sp., *Rumex* sp. and *Urtica* were used as
299 an indicator of anthropogenic activity.

300

301 In addition to pollen, non-pollen palynomorphs (NPP: microfossil remains of fungi, insect, algae and
302 cyanobacteria) were analyzed simultaneously with pollen from microscopic slides. NPPs provide
303 valuable additional proxy information for past disturbances and changes in the lake catchment (van
304 Geel, 2002). Identification of NPPs was based on van Geel (1998). Pollen and NPP data were plotted
305 using the C2 program (Juggins, 2003).

306

307 *2.5.3. Fossil bark beetle analysis*

308 For the analysis of bark beetles (Coleoptera: Curculionidae: Scolytinae), sediment was sieved over
309 100 µm mesh in order to retain all insect and botanical macro fossils (Hofmann, 1986; Birks, 2007).
310 Beetle remains were picked under a stereomicroscope with 50x magnification and bark beetles were
311 identified with the help of a small collection of Scolytinae species and an identification key of
312 Scolytinae of Czechoslovakia (Pfeffer, 1989). Primary (species feeding on healthy trees) and
313 secondary (species feeding on dying or dead trees) bark beetles were identified and their remains
314 were used for the reconstruction of the minimum number of individuals (MNI) per sample.

315

316 *2.5.4 Charcoal analysis and detection of fire events*

317 Macroscopic charcoal particles (> 200 µm) were used to detect local fires, where microscopic
318 charcoal provides a signal of regional fire history (Whitlock et al. 2001). For the reconstruction of
319 regional fires, microscopic charcoal was analyzed concurrently from the same microscopic slides used

320 for pollen and NPP identification. Opaque, sharp-edged particles ($> 5 \mu\text{m}$) were identified as charcoal
321 (Scott, 2010). The total concentrations (particles cm^{-3}) and influx (particles $\text{cm}^{-2} \text{yr}$) of microscopic
322 charcoal fragments were calculated for each sample. For the reconstruction of local fire events,
323 macroscopic charcoal was analyzed following the method adapted from Mooney and Tinner (2011).
324 Subsamples of $0.5\text{--}1 \text{ cm}^3$ were soaked in a 20 ml solution of sodium hexametaphosphate ($(\text{NaPO}_3)_6$)
325 and 10 ml of potassium hydroxide (KOH; 5 %). Samples were carefully sieved through a $250 \mu\text{m}$
326 mesh, and then bleached using a solution of 1 or 2 ml of NaOCl (8 %). After bleaching samples were
327 once more sieved through a $125 \mu\text{m}$ mesh. Macroscopic charcoal particles were first recorded under
328 a binocular microscope and then ImageJ (<https://imagej.nih.gov/ij/>) software was employed for
329 analyzing charcoal area measurements and counts using 8-bit images at a threshold of 137 greyscale
330 units (ie 137–255 greyscale units) following Halsall et al. (2018). The total concentrations and influx
331 of macroscopic charcoal area and counts were calculated for each sample.

332

333 CharAnalysis software, applying a signal-to-noise index (SNI) to separate peaks in the charcoal record
334 from background variability (Higuera 2009, 2010; Kelly et al., 2011) were used for assessing the
335 regional and local fire events. Microscopic charcoal concentrations (particles cm^{-3}) were used to
336 determine regional fires. Macroscopic charcoal concentrations (particles cm^{-3}) were used to assess
337 the local fire history. First both records were interpolated to mean temporal samples resolution and
338 then separated into a low-frequency background component (BCHAR) and a peak component using
339 the CharAnalysis software (Higuera, 2009). In both cases smoothing with LOWESS regression within a
340 100-year moving-window was applied to determine the background component. The peak
341 component was calculated as residuals between interpolated charcoal records and BCHAR ($C_{\text{peak}} =$
342 $\text{CHAR}_{\text{int}} - \text{BCHAR}$) and evaluated using the 99th percentile of a Gaussian mixture model in order to
343 separate fire events reflected by charcoal peaks from the background noise. Furthermore, detected
344 peaks in microscopic charcoal records were screened using minimum-count peak ($p = 0.05$) test in
345 CharAnalysis.

346
347
348
349
350
351
352
353
354
355
356
357
358
359
360
361
362
363
364
365
366
367
368
369
370
371

Determination of the macroscopic charcoal area has proven to be a reliable method for detection of local fires, when the number of charcoal particle counts is low (Ali et al., 2009; Halsall et al., 2018). Therefore macroscopic charcoal area measurements (the area of particles $\text{mm}^2 \text{cm}^{-2} \text{yr}$), were used as additional proxy to assess local fires.

2.5.5 Comparison of dendrochronological and palaeoecological data

To compare the palaeoecological records and the disturbance history based on dendrochronological records, all palaeoecological data (pollen, *Glomus* spores, sedimentary charcoal, bark beetles) were combined to 10-year bins corresponding the decadal resolution used in tree-ring based disturbance reconstruction (e.g. 1710–1720, 1720–1730, 1730–1740 etc.) and plotted using C2 –program (Juggins, 2003).

3. Results

3.1 Disturbance signal from dendrochronological data

The dendrochronological disturbance signal indicates that the most extensive disturbances occurred during the period of 1780–1830 CE (Fig. 3). The extensive, frequent disturbances affected all of the study plots within this period and removed most of the canopy cover on at least four of the six available plots (Appendix A.2). Two plots (plot 3 and 10) also experienced severe disturbance during the period of 1830–1860 CE. Other less severe (loss of $\geq 10\%$), localized disturbance events occurred regularly within the study period (e.g. in 1720s, 1740–1760, 1870s, 1900s, 1920s and 1980–1990s). The accuracy of the dendrochronological record is questionable before the 1760s due to the limited number of records available, however regional reconstruction from Šumava NP identifies regional disturbances during the 1690s, 1720s and 1740s (Čada et al., 2016a; see the paper for more detailed description of tree-ring based disturbance history).

372 [Figure 3.]

373

374 3.2 Disturbance signals from the lake sediments

375 *3.2.1 Trends in the physical properties and geochemistry*

376 In the physical properties measured for the Laka sediments 68.5% of the variation in a Principal
377 Components Analysis (PCA) is summarised on the first two components (Fig. 4). The geochemistry,
378 NIRS end member components and grain size parameters (d90, d50 and sorting) form three distinct
379 groupings in the PCA. Group 1 includes organic content and elements that strongly associate with
380 organic matter (Br, S and Cl). Group 2 associates NIRS-inferred biogenic silica with Si (mg m⁻¹)
381 measured by XRF, which suggests firstly that biogenic silica dominates these samples and second the
382 Si:Al ratio (Davies et al., 2015) should be a strong measure of biogenic silica that is independent of
383 NIRS-inferred biogenic silica. Coarser grains size and poor sorting also associate in part with biogenic
384 silica indicating that larger diatoms may be affecting grain size measurements for more organic older
385 samples. Group 3 (a+b) includes a large number of primarily minerogenic indicators including NIRS-
386 inferred mineral content and a series of lithogenic elements (e.g. Al, K, Zr, Ca and Ti).

387

388 [Figure 4.]

389

390 The cluster analysis of the physical properties highlights a series of major stratigraphical changes
391 through the last 800 years and provides a basis for zoning the sediment sequence (Fig. 5). There is
392 some separation with Group 3 with elements Cu, Pb, P and As plotting higher on PC2 closer to the
393 organic Group 1, the more easily remobilized elements (Al, Zn and Cr) plot lower on PC2, with the
394 more stable elements in the middle (Ti, Zr, K). There is a strong stratigraphical order to the
395 distribution of samples within the PCA progressing between the organic Zones 1, 3a and 4 with
396 abundant biogenic silica, and Zones 2 and 3b a mix of organic and mineral matter (Fig. 5). The
397 transition to Zones 5 and 6 reflects a substantial shift in the erosion regime in the catchment

398 producing limnic muds composed dominantly of minerogenic sediment and containing less organic
399 and diatomaceous material. Zone 7 shows evidence for a reduction in minerogenic material with
400 more diatom-rich sediments. Zone 8, the most recent sediments, plot as outliers in the PCA with
401 fluctuations in concentrations of biogenic silica, and a switch to lithogenic elements of the more
402 easily mobilized variety (Al, Zn and Cr).

403

404 [Figure 5.]

405

406 *3.2.2 Physical properties and geochemistry*

407 *Zone 1 (1200–1265 CE)*: has moderately low minerogenic content, but without being particularly
408 inorganic. Interpretation of the NIRS and Si:Al ratios reflect high concentrations of biogenic silica (Fig.
409 5). Laka appears quite productive and has a relatively stable catchment limiting the flux of
410 minerogenic materials. *Zone 2 (1265–1395 CE)*: begins with a sharp increase in mineral and organic
411 content, with sharp declines in biogenic silica. Concentrations of the detrital lithogenic elements all
412 increase mirrored by increases in grain size. The d₉₀ (µm) displays a series of peaks showing coarse
413 in-wash events that resemble flood or similar high-energy events. The catchment-lake area ratio is
414 large and flood in wash is a plausible mechanism (Schillereff et al., 2015). Lithogenic elements are not
415 uniform in their concentration, with broad multi-decade peaks early and late in zone 2. Organic
416 content for the most part varies inversely with the lithogenic elements. *Zone 3 (1395–1490 CE)*:
417 comprises two stages, an early 3a with abundant biogenic silica content which increases at the
418 expense of both mineral and organic content. This relationship reverses with 3b comprising a
419 pronounced minerogenic layer. Lithogenic elements follow the trends in the total mineral content.
420 Sediment grain size fluctuates reflecting a continued contribution of higher energy in- wash events.
421 Declines in the degree of sorting, however resemble patterns in biogenic silica indicating a possible
422 contribution from diatoms to the grain size spectra. *Zone 4 (1490–1610 CE)*: is dominated by peaks in
423 the Si:Al ratio and biogenic silica increasing to > 30 % of the sediment initially and latterly climbing to

424 maxima close to 50 %. These increases are at the expense of sharp declines in mineral content and
425 lithogenic elements. There is no inverse relationship with patterns in organic content, which declines
426 by 10 % through the zone. The sediment reflects a relatively stable catchment limiting the flux of
427 minerogenic materials to the lake and the lake is very productive. *Zone 5 (1610–1785 CE)*: is marked
428 by the most substantial changes in the sequence, with organic content falling to < 10 % and mineral
429 content increasing to > 90 %. NIRS-inferred biogenic silica and the Si:Al ratio suggest either an
430 absence of algae or dissolution of diatoms. We exclude masking of a diatom signal by the increased
431 flux of mineral matter, because Si and Al are in ratio. There is increase in lithogenic elements
432 throughout the zone. Higher energy in-wash event (~18 layers) are represented by d90 peaks that
433 extend into the fine sand and by poorer sorting of these coarse units. In summary, the catchment has
434 shifted to a more erodible condition, and higher energy flows drove the sharper peaks in coarser
435 minerogenic influx. *Zone 6 (1785–1860 CE)*: begins with declines in concentrations of lithogenic
436 elements and a minor dip in the total mineral content. These changes reflect greater organic content,
437 with little or no change in the proportion of biogenic silica. This recovery or increasing catchment
438 stability required to reduce the supply of lithogenic elements is short-lived and followed by further
439 layer of coarse sediment enriched with K, Zr and P denoting a further erosion episode. *Zone 7 (1860–*
440 *1910 CE)*: is unusual in commencing with falls in all lithogenic elements except for Si, a phenomenon
441 often associated with diatom rich sediments, but here NIRS-inferred diatoms and Si:Al ratio are both
442 low. Grain size increases sharply and so the unit comprises relatively pure quartz sand. Latterly, the
443 mineral content falls sharply, lithogenic elements continue at low concentrations, there is increased
444 organic content and a spike in biogenic silica, which is perhaps a lagged response by algal
445 communities in the lake to the influx of quartz sand to the lake. *Zone 8 (1910–2015 CE)*: is marked by
446 relatively slow rates of sediment accumulation and in the early part a sharp in-wash layer dominated
447 by increases in all lithogenic elements. The product of greater erosion in the catchment, this layer
448 contains finer grain sizes than the Zone 7 quartz-dominated event, and it suppresses both the
449 biogenic silica and organic content. The last 50 years show a stabilization of the catchment reflect by

450 declines across all lithogenic elements, increasing the organic and biogenic silica content. There is
451 minor mineral-rich layer near the top of the core profile.

452

453 The physical properties show substantial shifts in the flux of materials from catchment to the lake.
454 These take the form of shifts in the baseline chemistry and grain size, but also differing event scale
455 dynamics with greater frequency of in-wash layers/spikes, probably floods, during the extreme
456 erosive episode 1600–1790 CE. Together the physical properties show short-lived erosive episodes
457 1250–1300, 1340–1400, 1450–1500 and around 1550 CE, before a major regime change 1600–1790
458 and 1825–1860 CE. The peaks in minerogenic sediment supply reflect some form of catchment
459 disturbance, most likely perturbation of the forest cover; with the intervening lulls in minerogenic
460 sediment reflect system recovery. The last century shows slower rates of sediment accumulation but
461 includes a further minerogenic unit 1900–1950 CE before some recovery and a further minerogenic
462 influx event towards the top of the core.

463

464 3.2.3 Palynological records

465 Spruce was the dominant tree taxa in the forest vegetation during the last 800 years, with beech and
466 fir as minor components. Forest composition remained relatively constant during 1200–1900 CE and
467 most notable changes occurred during the 20th century. Pollen record demonstrates the highest
468 average proportion (30 %) of *Picea* pollen from 1500 to 1610 CE (Fig. 6). There is circa 10 %
469 momentarily drop around 1630 CE, after which the values stay roughly at 25 % until the end of the
470 19th century. During the last 100 years of the record proportion of *Picea* pollen fluctuated between
471 18–30 %, with lowest values at 1920s, 1930s and 1990s and highest values at 1900s and 1960s. *Fagus*
472 pollen had the second highest values of an average of 15 % proportion of the forest composition
473 during 1500–1900 CE. Most notable changes in *Fagus* pollen record occurred during the last 100
474 years, when the highest *Fagus* pollen values (12–14 %) coincided with the decline in *Picea* pollen
475 around 1930–40s. The highest values (8–10 %) of *Abies* pollen occurred during the first half of the

476 record from 13th to 16th century, followed by a gradual decline towards the present, especially
477 during the last 100 years of the record. The increase in the pollen proportion of light demanding
478 early successional taxa, such as *Acer*, *Populus*, *Salix*, *Sorbus*, *Epilobium*, and *Pteridium* coincides with
479 the decrease in the main tree taxa during the last 100 years indicating forest openness. Proportions
480 of herbs and human indicator taxa, such as Cerealia-type, *Secale cereale*, *Rumex* sp. and *Plantago* sp.,
481 increased slightly from 16th century with a clear increase during the 20th century, indicating the
482 opening of the landscape. More detailed pollen diagram can be found in Appendix A.3.

483

484 *Glomus* fungal spores were used as an additional indicator of soil erosion, possibly caused by
485 disturbances in lake catchment (van Geel, 2002). Increase in influx of *Glomus* fungal spores indicating
486 enhanced soil erosion of topsoil in the lake catchment occur at 1350–1400, 1450s, 1520s, between
487 1600–1780s, 1860s and 1950s (Fig. 6).

488

489 [Figure 6.]

490

491 3.2.3 Bark beetles

492 The number of insect remains is typically low due to the small volume samples analyzed throughout
493 the lake sediment record resulting in mostly one or zero individuals of Scolytinae per sample. Both
494 primary and secondary bark beetle remains were found throughout the core. The top part of the
495 core from 1620 CE to the present (0–255 cm) contained notably higher amounts of beetle remains
496 than the lower part (255–322 cm) of the core. Remains of *Ips typographus*, the species causing the
497 most extensive mortality of Norway spruce, were found at 1270, 1290, 1630, 1700, 1800, 1880 and
498 1950 CE (Fig. 6). Remains from other primary bark beetles feeding on Norway spruce, *Pityogenes*
499 *chalcographus*, *Pityogenes conjunctus*, *Polygraphus poligraphus* and *Polygraphus subopacus*, were
500 found throughout the core but mainly between 1620–1820 CE. The highest occurrence of primary
501 bark beetles in single samples was found during the 1800s, where *Ips typographus* appeared

502 together with *Polygraphus poligraphus* and *P. subopacus*. Remains of secondary bark beetles
503 consisted of a variety of genera, attacking dead or dying conifer trees. In general, occurrences of
504 secondary bark beetles coincided with primary bark beetles or shortly after. A detailed list of the
505 identified Scolytinae species can be found in Appendix A.4.

506

507 3.2.4 Fire history

508 The amount of sedimentary charcoal is relatively low in both micro- and macroscopic charcoal
509 records, and in the macroscopic area measurements during the last 800 years (Fig. 6). All records
510 show increasing values from 1600s onwards. Results from CharAnalysis show that average SNI values
511 were above 3.0 for both micro- and macroscopic charcoal count records demonstrating the
512 suitability of both records to the peak detection analysis. Ten significant peaks in the microscopic
513 charcoal were recorded in Šumava NP during the last 800 years. Highest peak magnitude in
514 microscopic charcoal was recorded at 1710 and 1770 CE indicating more extensive regional (longer
515 distance from the lake) fire events. In macroscopic charcoal record four significant charcoal peaks
516 were recorded indicating possible fire events at 1710, 1750, 1900 and 1980 CE in the vicinity of the
517 Laka. The macroscopic charcoal area measurements show an slight increase around 1700 and 1750
518 CE and between 1900–1910 CE corresponding with the peaks in macroscopic charcoal counts.
519 However, there is a peak in macroscopic charcoal area measurements at 1840 CE that is not detected
520 in the macroscopic charcoal particle concentrations. A more detailed reconstruction of fire history
521 and the results of CharAnalysis can be found in Appendix A.5.

522

523 4. Discussion

524 4.1 Increasing disturbances from 1600s

525 Multidisciplinary dataset of palaeoecological and dendrochronological records demonstrated
526 reoccurring disturbances in central European mountain spruce forest during the last 800 years (Fig.
527 6). Increases in *Glomus* spores together with the increase in lithogenic elements from 1600s suggest

528 changes to the catchment erosion regime. Coarse laminations in the more minerogenic episodes
529 reflect that higher flows (floods) are interacting with a landscape that is in general more susceptible
530 to erosion. This change coincides with the increase in sedimentary charcoal records and with the
531 continuous occurrence of fossil bark beetle remains. This change in the erosion regime is most likely
532 triggered by an increase in disturbance rate in the study area from 1600s. Tree-ring records
533 demonstrate period of severe disturbances in the lake surroundings between 1780–1820 CE.
534 Sedimentary records reveal that the period of more severe and/or frequent disturbances started at
535 the beginning of the 17th century. There is no local tree-ring data for the 17th century, but the
536 regional disturbance reconstruction from whole Šumava region demonstrated potentially extensive
537 disturbance event around 1620s (Čada et al., 2016a). While disturbance reconstruction based on
538 tree-ring records and physical proxies reflecting the erosional events give an indication of the
539 occurrence and timing of the disturbance events around the lake catchment, fossil bark beetle
540 remains, and charcoal records provide insights for the possible causes of the disturbances.

541

542 Morris et al. (2015) suggested that even low numbers of fossil bark beetle remains in lake sediments
543 may indicate disturbances and it is plausible that the continuous presence of fossil bark beetle
544 remains, although in low numbers, from 1600s is linked to increasing frequency of bark beetle
545 disturbances. Presence of three different species of primary and two species of secondary bark
546 beetle in fossil record between 1700–1720 CE coincides with the historical documents recording
547 insect outbreaks in the area around 1720s (Zatloukal, 1998; Brádzil, 2004; Jelínek, 2005). The highest
548 number of different primary and secondary bark beetle species around 1800s coincide with the
549 period of maximum disturbance indicated in the tree-ring based disturbance signal and sedimentary
550 records. It is plausible that disturbances in the early 1800s might have resulted from the joint effect
551 of insect outbreak indicated in the fossil record and windthrows documented in the archival
552 documents (see Čada et al., 2016a). The effect of outbreaks on the amount of fossil bark beetle
553 remains accumulating into lake sedimentary basin is still unknown. Therefore, it could be only

554 speculated that the presence of fossil bark beetles during the disturbance events at 1380–1400 and
555 1510–1530 CE, indicated by the soil erosion (increased flux of lithogenic elements and *Glomus*
556 spores), could have been at least partly caused by bark beetle outbreaks. The periods of absence of
557 bark beetle fossils before 1600s, coincide with the periods of low disturbance rate indicated by both
558 tree-ring and sedimentary records. Bark beetle population were probably smaller during these
559 periods and did not cause more extensive tree mortality. This may be, because bark beetle outbreaks
560 are not only triggered by favorable climatic conditions, such as warm and dry weather, but also by
561 stand structural characteristics (older and bigger trees are more sensitive to bark beetles) and related
562 windthrows (Seidl et al., 2011; Thom et al., 2013). In general, these results suggest that bark beetle
563 outbreaks have been an important part of the disturbance regime in mountain spruce forests for a
564 long time and that windstorms and insect outbreaks are the main and intimately related disturbance
565 agents in central European mountain spruce forests (e.g. Svoboda et al., 2013; Seidl et al., 2014; Čada
566 et al., 2016a). We also found that these disturbance agents may produce a substantial response in
567 erosion regime of the affected areas. Comparison of the fossil bark beetle remains together with
568 dendrochronological reconstruction is promising and may provide more exact information about past
569 bark beetle outbreaks, but further development of the method with more extensive dataset is
570 needed.

571

572 Compared to windthrows and bark beetle outbreaks, fire disturbances have not been studied
573 intensively in central European mountain spruce forest probably because there are very few known
574 recent natural fires in these forests (Feurdean et al., 2017). Our sedimentary disturbance record
575 revealed the presence of fires in the history of the studied area and it suggests increased fire activity
576 from the 1600 CE onwards. The more pronounced increase in microscopic charcoal compared to
577 macroscopic charcoal most probably indicates regional fires, rather than local fires in the lake
578 catchment. However, macroscopic charcoal records suggest four local fire events in the lake
579 catchment from which the significant peak around 1800 CE is recorded in both micro- and

580 macroscopic charcoal records, and coincides with the period of the most severe disturbances
581 indicated by tree-ring records, with erosional indicators and with the highest number of bark beetle
582 taxa. As there are no significant changes in forest composition in connection to these events, it is
583 likely that no substantial stand-replacing fires, but rather small and very local fires occurred in the
584 study area. Fires may have been connected to the increasing fuel load from windthrows and bark
585 beetle infested dying trees. Similar co-occurrence of bark beetle outbreak and fires were observed
586 after the severe windthrow at 2004 in Tatra mountains (Fleischer et al., 2017). However, it is also
587 important to note that these fires may have been also connected to the increased human influence
588 in the area. Although, fires have been scarce around the study site during the last millennia, our
589 results together with a recent study by Carter et al. (2018) demonstrated that fires have been part of
590 the long-term disturbance dynamics in Šumava NP. Furthermore, the recent report of European
591 commission EIP-AGRI focus group (2019) identified the increasing fire risk in temperate continental
592 zone and mountain forests as one of the probable climate change impacts. Therefore, it is vital to
593 acknowledge the role of fires in the past disturbance history and the probable future role of fires in
594 the management plans of the temperate mountain spruce forests.

595

596 In general, the long-term disturbance dynamics derived from both dendrochronological and
597 palaeoecological records demonstrate the co-occurrence of multiple disturbance factors such as
598 windthrows, bark beetles and fires. Similar interaction of different disturbance agents has been
599 reported also in previous studies (e.g. Brunelle et al., 2008; Holeksa et al., 2016; Nagel et al., 2017;
600 Šoltěs et al., 2010). Hence, the future forest management and conservation strategies should
601 acknowledge that multiple disturbance factors, such as windthrows, bark beetles, and fires may
602 occur simultaneously creating a complex disturbance regime in mountain forests affecting the forests
603 composition and structure.

604

605 4.2. Stable forest composition until the end of the 20th century

606 Despite the fact that the studied spruce forest was subjected to relatively extensive disturbances
607 during 1600–1900 CE, only minor changes in the pollen composition were recorded in this period.
608 However, the most notable changes in pollen composition that could relate to forest disturbances
609 were recorded at the beginning of the 20th century, when only small disturbance events were
610 indicated by dendrochronological analyses. The decline in *Picea* pollen during the 1930s and 1970s
611 together with an increase of landscape openness indicators may be connected to the windstorms
612 recorded in historical documents (Brádzil, 2004).

613

614 More intensive and/or proximal anthropogenic disturbance near the lake during last 100 years could
615 also explain the shift in pollen composition. Current forest structure indicates localized clearings and
616 management in the surrounding forest and along the lake shore, this coincides with an increase of
617 cultivated plants observed in the pollen taxa during the 20th century. It is also plausible that human
618 induced air pollution peaked in the region during the 1950–1980s affected the physiology of the
619 mature trees (Kopáček et al., 2001; Čada et al., 2016b), which may have resulted in lower pollen
620 production and hence more notable changes in the pollen records corresponding to disturbance
621 events during the last 100 years.

622

623 4.3 Integration of dendrochronological and sedimentary data

624 In the integration of tree-ring and sedimentary data, the biggest challenge lies in the unambiguous
625 temporal and spatial correlation of these two different datasets. We expected that the disturbance-
626 related mortality of mature trees, indicated by tree-ring records and resulting in a likely decrease in
627 spruce trees, would be accompanied by a decrease in the proportion of spruce pollen in the
628 sedimentary pollen record. However, pollen records of the main tree taxa did not indicate
629 substantial compositional changes during the major disturbance events revealed by
630 dendrochronology around 1800s. There are multiple reasons for this discrepancy. It is probable that
631 although Laka is a small lake, the relative source area of pollen extends beyond the lake catchment

632 due to the strong upscaling winds in the mountain region that may bring regional rather than local
633 pollen signals (e.g. Bunting et al., 2008; van der Knaap, 2010), whereas the disturbance signal from
634 tree-rings is very local. The relatively high proportion of *Corylus* pollen supports this notion, as the
635 closest hazel population is located at a lower elevation circa 1–2 km from the study site. Whereas the
636 pollen record reflects the vegetation from all directions surrounding Laka, the tree-ring record based
637 on 6 study plots is highly localized and all plots are located on the slope above the southern edge of
638 the lake in the old growth stand. Therefore, the source area for the pollen record derived from a lake
639 sediments and the disturbance signal from individual tree-ring study plots may have notably different
640 spatial scale.

641

642 Other explanations for the lack of any clear response between the pollen record and the extensive
643 disturbance events based on tree-ring data may be related to pollen production. It is possible that
644 the canopy opening was only moderate, when the whole canopy area is considered and that the
645 pollen production in remaining trees increased in response to disturbance due to increased light and
646 nutrient availability, or that the trees in the closest proximity of the lake might have survived
647 disturbance events and subsequently influence the pollen record. Furthermore, as windthrows and
648 bark beetle outbreaks kill mainly the mature trees, the younger, surviving trees continue or quickly
649 start to produce pollen and hence there may be a weaker signal in the pollen records compared to
650 e.g. notable changes in the pollen composition seen after severe stand-replacing fire event. It is
651 therefore probable that patchy forest disturbances driven primarily by wind and insect outbreaks
652 (Čada et al., 2016a) are not necessarily reflected in the main tree pollen taxa derived from lake
653 sediments.

654

655 From our knowledge, this is the first study to compare tree-ring based and sedimentary disturbance
656 records in order to construct more precise disturbance reconstruction. Although, integration of these
657 two different data sets can be challenging, the information derived from both records are

658 complementing and when combined can provide valuable insights into the cause, extent and
659 consequences of the disturbance events. It is noteworthy that sedimentary records that most likely
660 have originated from the lake catchment, such as fossil beetle remains indicating bark beetle
661 outbreaks, macroscopic charcoal indicating local fires, high values of *Glomus* spores together with
662 increase in physical and geochemical properties indicating soil erosion, demonstrate similar trends to
663 those reconstructed using tree-ring data. This allows the interpretation of possible causes behind the
664 disturbance events indicated by tree-ring record. Furthermore, comparison of sedimentary records
665 to the tree-ring records demonstrated that all disturbances are not necessarily visible in the pollen
666 record, but may still have important impact on the forest structure, especially when caused by
667 disturbance agents that affect just specific age cohorts, such as windstorms or insect outbreaks.
668 Finally, with the palaeoecological and sedimentological records we were able to extend the
669 disturbance reconstruction beyond the length of the tree-ring chronology (age of tree generation)
670 and demonstrate changes in the disturbance regime, which were not detectable in the
671 dendrochronological records. In future, the challenges in the integration of multidisciplinary data
672 that have different spatial and temporal limitation could be overcome with using more local sampling
673 sites (e.g. small hollows) for palaeoecological data or more regional set of dendrochronological study
674 plots. To overcome the offset in the temporal resolution of the different records would require even
675 more high-resolution sedimentary records and high chronological control of the samples.

676

677 **5. Conclusions**

678 Comparison of disturbance records from multidisciplinary data can provide important insight into the
679 disturbance agents and the changes in forest composition. Multidisciplinary data demonstrate more
680 frequent disturbance events and heightened catchment erosion from the 1600s in the study area.
681 This suggests that there has been long-term shift in disturbance history, that could not have been
682 detected solely with dendrochronological record. Although, windstorms and insect outbreaks are

683 considered as main disturbance factors in the mountain spruce forest, the role of fires should not be
684 ignored in the future forest management and conservation strategies.

685

686 This study highlights the importance of spatial and temporal consideration when integrating
687 multidisciplinary datasets. We demonstrated that sedimentary proxies that originates from the lake
688 catchment appear to mirror patterns in the tree-ring based disturbance signal. As the spatial scale of
689 the datasets used may largely explain the discrepancies between palynological and tree-ring records,
690 there is need for developing more precise analytical methods to integrate dendrochronological,
691 sedimentological and palaeoecological data from spatially more constrained sites as from small
692 forest hollows or if lake sediment is used comparison should be conducted with more larger
693 dendrochronological data set.

694

695 **Authors' contributions**

696 NK, JLC (PI) and VČ conceived the idea and designed the study; NK, VČ, KH, NBS, MK, RCC, JFB, JLC
697 collected and produced the data. NK, VČ, RC and JLC did the data analysis. All authors participated to
698 the interpretation of data. NK led the writing of the manuscript. All authors contributed to the drafts
699 and gave approval for the publication of the final manuscript.

700

701 **Acknowledgements**

702 In regards the coring and processing the sedimentary data we want to thank John Boyle, Lauren
703 Boyle, Daniel Schillereff, Fiona Russell, Isaac Clear, Daniel Vondrák, Tereza Opravilová, and Jolana
704 Tátošová. In regard to dendrochronological records we would like to thank Tomáš and Bohuslav
705 Koutecký for field sample collection, Jonny F. Pena and others for laboratory measurement. We
706 would also like to thank the Šumava National Park authorities for research permission in the national
707 park and allowing us to retrieve sediment core from Lake Laka.

708

709 **Funding**

710 Financial support for this research was provided by the PEDECO project (number 16-23183Y) funded
711 by the Czech Science Foundation (GAČR). The involvement of Miloš Knížek was supported by the
712 Ministry of Agriculture of the Czech Republic, institutional support MZE-RO0118.

713

714 **Declaration of interests**

715 The authors declare that they have no known competing financial interests or personal relationships
716 that could have appeared to influence the work reported in this paper.

717

718 **References**

719

720 Ali, A.A., Higuera, P.E., Bergeron, Y., Carcaillet, C., 2009. Comparing fire-history interpretations based
721 on area, number and estimated volume of macroscopic charcoal in lake sediments. *Quaternary Res.*
722 *72*, 462–468. <https://doi.org/10.1016/j.yqres.2009.07.002>

723

724 Appleby, P.G., Nolan, P.J., Gifford, D.W., Godfrey, M.J., Oldfield, F., Anderson, N.J., Battarbee, R.W.,
725 1986. ^{210}Pb dating by low background gamma counting. *Hydrobiologia* *141*, 21–27.
726 <https://doi.org/10.1007/BF00026640>

727

728 Appleby, P.G., Oldfield, F., 1978. The calculation of ^{210}Pb dates assuming a constant rate of supply of
729 unsupported ^{210}Pb to the sediment. *Catena* *5*, 1–8. [https://doi.org/10.1016/S0341-8162\(78\)80002-2](https://doi.org/10.1016/S0341-8162(78)80002-2)

730

731 Appleby, P.G., Richardson, N., Nolan, P.J., 1991. ^{241}Am dating of lake sediments. *Hydrobiologia* *214*,
732 35–42. <https://doi.org/10.1007/BF00050929>

733

734 Beug, H-J., 2004. Leitfaden der Pollenbestimmung für Mitteleuropa und angrenzende Gebiete.
735 Friedrich Pfeil, German, pp. 542.

736

737 Birks, H.H., 2007. "Plant Macrofossil Introduction," In: S. A. Elias, Ed., *Encyclopedia of Quaternary*
738 *Science*, Elsevier, Vol. 3., pp. 2266-2288. doi:10.1016/B0-44-452747-8/00215-5

739

740 Blaauw, M., Christen, J.A., 2011. Flexible paleoclimate age-depth models using an autoregressive
741 gamma process. *Bayesian Anal.* 6, 457–474. doi:10.1214/11-BA618.
742

743 Blott, S. J., Pye, K., 2001. GRADISTAT: a grain size distribution and statistics package for the analysis
744 of unconsolidated sediments. *Earth Surf. Process.* 26, 1237–1248. <https://doi.org/10.1002/esp.261>
745

746 Bobek, P., Šamonil, P., Jamrichová, E., 2018. Biotic controls on Holocene fire frequency in a
747 temperate mountain forest, Czech Republic. *J. Quat. Sci.* 33(8),892–904.
748 <https://doi.org/10.1002/jqs.3067>
749

750 Boyle, J.F., 1995. A simple closure mechanism for a compact, large-diameter, gravity corer. *J*
751 *Paleolimnol* 13(1), 85–87. doi:10.1007/BF00678113.
752

753 Boyle, J.F., Chiverrell, R.C., Schillereff, D., 2015. Approaches to water content correction and
754 calibration for μ XRF core scanning: comparing X-ray scattering with simple regression of elemental
755 concentrations. *Micro-XRF Studies of Sediment Cores*, 373–390. [https://doi.org/10.1007/978-94-017-](https://doi.org/10.1007/978-94-017-9849-5_14)
756 [9849-5_14](https://doi.org/10.1007/978-94-017-9849-5_14)
757

758 Brázdil, R., Dobrovolný, P., Štekl, J., Kotyza, O., Valášek, H., Jež, J., 2004. History of Weather and
759 Climate in the Czech Lands VI: Strong Winds. Masaryk University, Brno.
760

761 Brunelle, A.R., Rehfeldt, J., Bentz, B.J., Munson, A.S., 2008. Holocene records of *Dendroctonus* bark
762 beetles in high elevation pine forests of Idaho and Montana, USA. *For. Ecol. Manag.* 255, 836–846.
763 <https://doi.org/10.1016/j.foreco.2007.10.008>
764

765 Bunting, M.J., Twiddle, C.L., Middleton, R., 2008. Using models of pollen dispersal and deposition in
766 hilly landscapes: Some possible approaches. *Palaeogeogr. Palaeoclimatol. Palaeoecol.* 259, 77–91.
767 <https://doi.org/10.1016/j.palaeo.2007.03.051>
768

769 Čada V., Svoboda, M., Janda, P., 2013. Dendrochronological reconstruction of the disturbance history
770 and past development of the mountain Norway spruce in the Bohemian Forest, central Europe. *For.*
771 *Ecol. Manag.* 295, 59–68. <https://doi.org/10.1016/j.foreco.2012.12.037>
772

773 Čada V., Morrissey, R.C., Michalova, Z., Bacě, R., Janda, P. Svoboda, M., 2016a. Frequent severe
774 natural disturbances and non-equilibrium landscape dynamics shaped the mountain spruce forest in
775 central Europe. *For. Ecol. Manag.* 363, 169–178. <https://doi.org/10.1016/j.foreco.2015.12.023>
776

777 Čada, V., Šantrůčková, H., Šantrůček, J., Kubištová, L., Seedre, M., Svoboda, M., 2016b. Complex
778 physiological response of Norway spruce to atmospheric pollution–decreased carbon isotope
779 discrimination and unchanged tree biomass increment. *Front. Plant Sci.* 7, 805.
780 <https://doi.org/10.3389/fpls.2016.00805>
781

782 Carter, V.A., Moravcová, A., Chiverrell, R.C., Clear, J.L., Finsinger, W. Dreslerová, D., Halsall, K., Kuneš,
783 P., 2018. Holocene-scale fire dynamics of central European temperate spruce-beech forests. *Quat.*
784 *Sci. Rev.* 191, 15–30. <https://doi.org/10.1016/j.quascirev.2018.05.001>
785

786 Cháb, J., Stráník, Z., Eliáš, M., 2007. Geological Map of the Czech Republic 1:500,000. Czech
787 Geological Survey, Prague
788

789 Christen, J.A., Perez, S.E., 2009. A New Robust Statistical Model for Radiocarbon Data. *Radiocarbon*
790 51, 1047–1059. <https://doi.org/10.1017/S003382220003410X>
791

792 Davies, S., Lamb, H., Roberts, S., 2015. Micro-XRF Core Scanning in Palaeolimnology: Recent
793 Developments. In: Croudace I., Rothwell R. (eds) *Micro-XRF Studies of Sediment Cores.*
794 *Developments in Paleoenvironmental Research*, vol 17. Springer, Dordrecht.
795 https://doi.org/10.1007/978-94-017-9849-5_7
796

797 Drobyshev, I., Niklasson, M., Angelstam, P., 2004. Contrasting tree-ring data with fire record
798 in a pine-dominated landscape in the Komi Republic (Eastern European Russia): recovering a
799 common climate signal. *Silva Fenn.* 38(1),43–53. <https://doi.org/10.14214/sf.434>
800

801 Edwards, M.E., Dunwiddie, P.W., 1985. Dendrochronological and Palynological Observations on
802 *Populus Balsamifera* in Northern Alaska, U.S.A. *Arct Antarct Alp Res.* 17(3),271–277.
803 [10.1080/00040851.1985.12004035](https://doi.org/10.1080/00040851.1985.12004035)
804

805 Faegri, K., Kaland, P.E., Kzywinski, K., 1989. *Textbook of Pollen Analysis.* Wiley, New York.
806

807 Feurdean, A., Florescu, G., Vanni re, B., Tan au, I., O'Hara, R.B., Pfeiffer, M., Hutchinson, S.M.,
808 Mariusz Ga ka, M., Moskal-del Hoyo, M., Hickler, T., 2017. Fire has been an important driver of forest
809 dynamics in the Carpathian Mountains during the Holocene. *For. Ecol. Manag.* 389,15–26.
810 <https://doi.org/10.1016/j.foreco.2016.11.046>
811
812 Fleischer, P., Pichler, V. , Fleischer P. Jr, Holko, L., Mali, F., Gomoryova, E., Cudlin, P., Holeksa, J.,
813 Michalova, Z., Homolova, Z., Strelcova, K., Hlava , P., 2017. Forest ecosystem services affected by
814 natural disturbances, climate and land-use changes in the Tatra Mountains. *Clim. Res.* 73, 57–71.
815 <https://doi.org/10.3354/cr01461>
816
817 Van Geel, B., 1998. *A Study of Non-Pollen Objects in Pollen Slides.* Utrecht.
818
819 Van Geel, B., 2002. Non-pollen palynomorphs. *In* J. P. Smol, H. J. B. Birks & W. M. Last (eds.), 2001.
820 *Tracking Environmental Change Using Lake Sediments. Volume 3: Terrestrial, Algal, and Siliceous*
821 *indicators.* Kluwer Academic Publishers, Dordrecht, The Netherlands. [https://doi.org/10.1007/0-306-](https://doi.org/10.1007/0-306-47668-1_6)
822 [47668-1_6](https://doi.org/10.1007/0-306-47668-1_6)
823
824 Halsall, K.M., Ellingsen, V.M., Asplund, J., Bradshaw, R.H.W., Ohlson, M., 2018. Fossil charcoal
825 quantification using manual and image analysis approaches. *The Holocene* 28, 1345–1353.
826 <https://doi.org/10.1177/0959683618771488>
827
828 Helama, S., Seppa, H., Bjune, A.E., Birks, H.J.B. 2012. Fusing pollen-stratigraphic and dendroclimatic
829 proxy data to reconstruct summer temperature variability during the past 7.5 ka in subarctic
830 Fennoscandia. *J Paleolimnol* 48,275–286. <https://doi.org/10.1007/s10933-012-9598-1>
831
832 Higuera, P.E., Sprugel, D.G. Brubaker, L.B., 2005. Reconstructing fire regimes with charcoal from
833 small-hollow sediments: a calibration with tree-ring. *The Holocene* 15, 238–251.
834 <https://doi.org/10.1191/0959683605hl789rp>
835
836 Higuera, P.E., Brubaker, L.B., Anderson, P.M., Hu, F.S., Brown, T.A., 2009. Vegetation mediated the
837 impacts of postglacial climatic change on fire regimes in the south-central Brooks Range, Alaska. *Ecol.*
838 *Monog.* 79, 201–219. <https://doi.org/10.1890/07-2019.1>
839

840 Higuera, P.E., Gavin, D.G., Bartlein, P.J., & Hallet, D.J. 2010. Peak detection in sediment-charcoal
841 records: impacts of alternative data analysis methods on fire-history interpretation. *International*
842 *Journal of Wildland Fire*, 19, 996–1014. Doi:10.1071/WF09134.

843

844 Hofmann, W., 1986. "Chironomid analysis," In: Berglund, B. (Ed), *Handbook of Holocene*
845 *palaeoecology and palaeoecology*. New York, Wiley, pp 715–727.

846

847 Holeksa, J., Jaloviar, P., Kucbel, S., Saniga, M., Svoboda, M., Szewczyk, J., Jerzy Szwagrzyk, J., Zielonka,
848 T., Żywiec, M., 2017. Models of disturbance driven dynamics in the West Carpathian spruce
849 Forests. *For. Ecol. Manag.* 388, 79–89. <https://doi.org/10.1016/j.foreco.2016.08.026>

850

851 Holeksa, J., Zielonka, T., Żywiec, M., Fleischer, P., 2016. Identifying the disturbance history over a
852 large area of larch–spruce mountain forest in Central Europe. *For. Ecol. Manag.* 361, 318–327.
853 <https://doi.org/10.1016/j.foreco.2015.11.031>

854

855 Janda, P., Trotsiuk, V., Mikoláš, M., Bače, R., Nagel, T.A., Seidl, R., Seedre, M., Morrissey, R.C., Kucbel,
856 S., Paloviar, P., Jasík, M., Vysoký, J., Šamonil, P., Čada, V., Mrhalová, H., Lábusová, J., Nováková, M.H.,
857 Rydval, M., Matějů, L., Svoboda, M., 2017. The historical disturbance regime of mountain Norway
858 spruce forests in the Western Carpathians and its influence on current forest structure
859 and composition. *For. Ecol. Manag.* 388, 67–78. <https://doi.org/10.1016/j.foreco.2016.08.014>

860

861 Jelínek, J., 2005. *Od jihočeských pralesůk hospodářským lesům Šumavy*. MZe ČR, ÚHÚL, Brandýs nad
862 Labem.

863

864 Juggins, S., 2003. *C2 user guide*. Software for ecological and palaeoecological data analysis and
865 visualization. University of Newcastle upon Tyne, Newcastle.

866

867 Kelly, R., Higuera, P.E., Barrett, C.M., Hu, F.S., 2011. A signal-to-noise index to quantify the potential
868 for peak detection in sediment-charcoal records. *Quaternary Res.* 75, 11–17.
869 doi:10.1016/j.yqres.2010.07.011.

870
871 van der Knaap, W.O., van Leeuwen, J.F.N., Svitavská-Svobodová, H., Pidek, I.A., Kvavadze, E.,
872 Chichinadze, M., Giesecke, T., Kaszewski, B.M., Oberli, F., Kalniņa, L., Pardoe, H.S., Tinner, W.,
873 Ammann, B., 2010. Annual pollen traps reveal the complexity of climatic control on pollen
874 productivity in Europe and the Caucasus. *Veget Hist Archaeobot* 19, 285–307.
875 <https://doi.org/10.1007/s00334-010-0250-6>
876
877 Kopáček, J., Veselý, J. Evzen Stuchlík, E., 2001. Sulphur and nitrogen fluxes and budgets in the
878 Bohemian Forest and Tatra Mountains during the Industrial Revolution (1850-2000). *Hydrol. Earth*
879 *Syst. Sci.* 5(3),391–405.
880
881 Kozák, J., 2010. Soil Atlas of the Czech Republic. Czech University of Life Sciences, Prague, Prague,
882
883 Kozáková, R., Pokorný, P., Peša, V., Danielisová, A., Čuláková, K., Svitavská Svobodová, H., 2015
884 Prehistoric human impact in the mountains of Bohemia. Do pollen and archaeological data support
885 the traditional scenario of a prehistoric “wilderness”? *Rev Palaeobot Palyno* 220,29–43.
886 <https://doi.org/10.1016/j.revpalbo.2015.04.008>
887
888 Kulakowski, D., Seidl, R., Holeksa, J., Kuuluvainen, T., Nagel, T.A., Panayotov, M., Svoboda, M., Thorn,
889 S., Vacchiano, G., Whitlock, C., Wohlgemuth, T., Bebi, P., 2017. A walk on the wild side: Disturbance
890 dynamics and the conservation and management of European mountain forest ecosystems. *For. Ecol.*
891 *Manag.* 388,120–131. <https://doi.org/10.1016/j.foreco.2016.07.037>
892
893 Lorimer, C., Frelich, L., 1989., A methodology for estimating canopy disturbance frequency and
894 intensity in dense temperate forests. *Can. J. For. Res.* 19,651–663. <https://doi.org/10.1139/x89-102>
895
896 McLachlan, J.S., Foster, D.R. Menalled, F. 2000. Anthropogenic ties to late-successional structure and
897 composition in four New England hemlock stands. *Ecology* 81(3),717–733.
898 [https://doi.org/10.1890/0012-9658\(2000\)081\[0717:ATLSS\]2.0.CO;2](https://doi.org/10.1890/0012-9658(2000)081[0717:ATLSS]2.0.CO;2)
899
900 Mentlík, P., Minár, J., Břízová, E., Lisá, L., Tábořík, P., Stacke, V., 2010. Glaciation in the surroundings
901 of Práslské Lake (Bohemian Forest, Czech Republic). *Geomorphology* 117,181–194.
902 <https://doi.org/10.1016/j.geomorph.2009.12.001>
903

904 Mooney, S.D. and Tinner, W. 2011. The analysis of charcoal in peat and organic sediments. *Mires and*
905 *Peat* 7, 1–18.

906

907 Moore, P.D., Webb, J.A., Collinson, M.E., 1991. *Pollen Analysis*. Blackwell Scientific
908 Publications, Oxford.

909

910 Morris, J.L., Courtney Mustaphi, C.J., Carter, V.A., Watt, J., Derr, K., Pisaric, M.F.J., Scott Anderson, R.
911 and Brunelle, A.R., 2015. Do bark beetle remains in lake sediments correspond to severe outbreaks?
912 A review of published and ongoing research. *Quat. Int.* 387,72–86.
913 <https://doi.org/10.1016/j.quaint.2014.03.022>

914

915 Nagel, T.A., Mikac, S., Dolinar, M., Klopčič, M., Keren, S., Svoboda, M., Diaci, J., Andrej Boncina, A.,
916 Paulić, V. 2017. The natural disturbance regime in forests of the Dinaric Mountains: A synthesis of
917 evidence. *For. Ecol. Manag.* 388,29–42. <https://doi.org/10.1016/j.foreco.2016.07.047>

918

919 Neuhäuslová, Z., Moravec, J., 1998. *Map of Potential Natural Vegetation of the Czech Republic*.
920 Academia, Prague.

921

922 Niklasson, M., Lindbladh, M., Björkman, L., 2002. A long-term record of *Quercus* decline, logging and
923 fires in a southern Swedish *Fagus-Picea* forest. *J Veg Sci* 13,765–774. [https://doi.org/10.1111/j.1654-](https://doi.org/10.1111/j.1654-1103.2002.tb02106.x)
924 [1103.2002.tb02106.x](https://doi.org/10.1111/j.1654-1103.2002.tb02106.x)

925

926 Niklasson, M., Zin, E., Zielonka, T., Feijen, M., Korczyk, A.F., Churski, M., Samojlik, T., drzejewska
927 B., Gutowski, J.M. & Brzeziecki, B., 2010. A 350-year tree-ring fire record from Białowieża Primeval
928 Forest, Poland: implications for Central European lowland fire history. *J Ecol.* 98,1319–1329.
929 <https://doi.org/10.1111/j.1365-2745.2010.01710.x>

930

931 Pfeffer, A., 1989. *Kůrovcovití (Scolytidae) a jádrohlodovití (Platypodidae)*. Praha, Academia: 137.

932

933 Reimer, P., Bard, E., Bayliss, A., Beck, J., Blackwell, P., Ramsey, C., . . . Van der Plicht, J., 2013.
934 Selection and Treatment of Data for Radiocarbon Calibration: An Update to the International
935 Calibration (IntCal) Criteria. *Radiocarbon* 55(4), 1923–1945.
936 https://doi.org/10.2458/azu_js_rc.55.16955

937

938 Reyer C.P.O, Brouwers, N., Rammig, A., Brook, B.W., Epila, J., Grant, R.F., Holmgren, M., Langerwisch,
939 F., Leuzinger, S., Lucht, W., Medlyn, B., Pfeifer, M., Steinkamp, J., Vanderwel, M.C., Verbeeck, H.,
940 Villela, D.M., 2015. Forest resilience and tipping points at different spatio-temporal scales:
941 approaches and challenges. *J Ecol.* 103,5–15. <https://doi.org/10.1111/1365-2745.12337>
942

943 Russell, F.E., Boyle, J.F., Chiverrell, R.C., 2019. NIRS quantification of lake sediment composition by
944 multiple regression using end-member spectra. *J. Paleolimnol* 62,73–88.
945 <https://doi.org/10.1007/s10933-019-00076-2>
946

947 Schelhaas, M.J., Nabuurs, G.J., Schuck, A., 2003. Natural disturbances in the European forests in the
948 19th and 20th centuries. *Glob. Change Biol.* 9, 1620–1633. [https://doi.org/10.1046/j.1365-](https://doi.org/10.1046/j.1365-2486.2003.00684.x)
949 [2486.2003.00684.x](https://doi.org/10.1046/j.1365-2486.2003.00684.x)
950

951 Scott A.C., 2010. Charcoal recognition, taphonomy and uses in palaeoenvironmental analysis.
952 *Palaeogeogr. Palaeoclimatol. Palaeoecol.* 291,11–39. doi:10.1016/j.palaeo.2009.12.012.
953

954 Schillereff, D.N, Chiverrell, R.C., Croudace, I.W., Boyle, J.F., 2015. An Inter-comparison of μ XRF
955 Scanning Analytical Methods for Lake Sediments. In Croudace, I., Rothwell, R., (eds) *Micro-XRF*
956 *Studies of Sediment Cores. Developments in Paleoenvironmental research 17.* Springer, Dordrecht.
957 https://doi.org/10.1007/978-94-017-9849-5_24
958

959 Seidl, R., Schelhaas, M.-J., Lexer, M.J., 2011. Unraveling the drivers of intensifying forest disturbance
960 regimes in Europe. *Glob. Change Biol.* 17, 2842–2852. [https://doi.org/10.1111/j.1365-](https://doi.org/10.1111/j.1365-2486.2011.02452.x)
961 [2486.2011.02452.x](https://doi.org/10.1111/j.1365-2486.2011.02452.x)
962

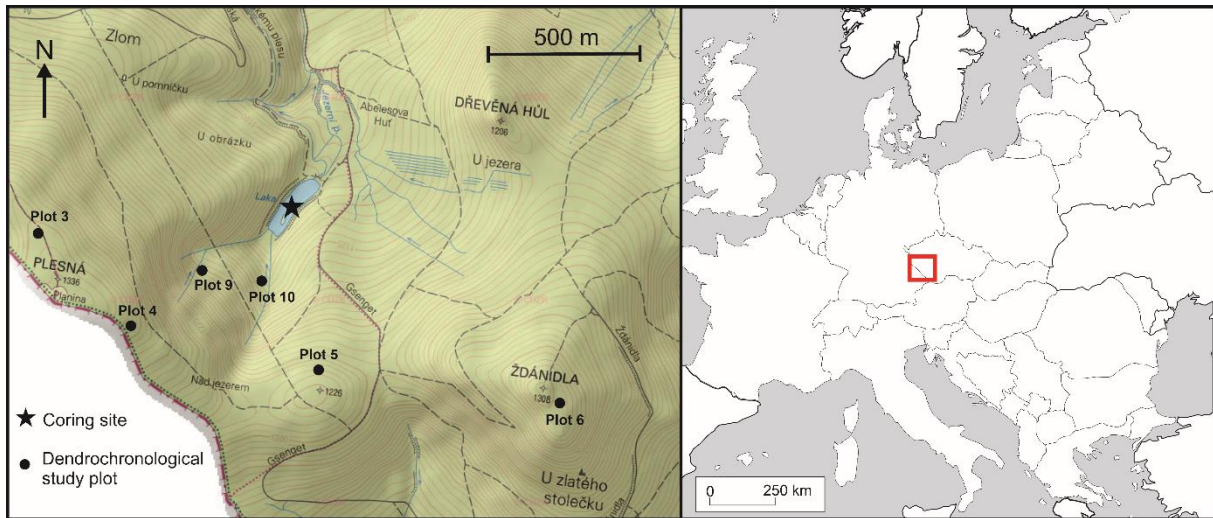
963 Seidl, R., Schelhaas, M.-J., Rammer W., Verkerk P.J., 2014. Increasing forest disturbances in Europe
964 and their impact on carbon storage. *Nat. Clim. Change* 4, 806–810.
965 <https://doi.org/10.1038/nclimate2318>
966

967 Šoltés, R., Školek, J., Homolová, Z., Kyselová, Z. 2010., Early successional pathways in the Tatra
968 Mountains (Slovakia) forest ecosystems following natural disturbances. *Biologia* 65(6),958–964.
969 <https://doi.org/10.2478/s11756-010-0110-y>
970

971 Stivrins, N., Aakala, T., Ilvonen, L., Pasanen, L., Kuuluvainen, T., Vasander, H., Gařka, M., Disbrey, H.R.,
972 Janis Liepins, J., Holmström, L. and Seppä, H., 2019. Integrating fire-scar, charcoal and fungal

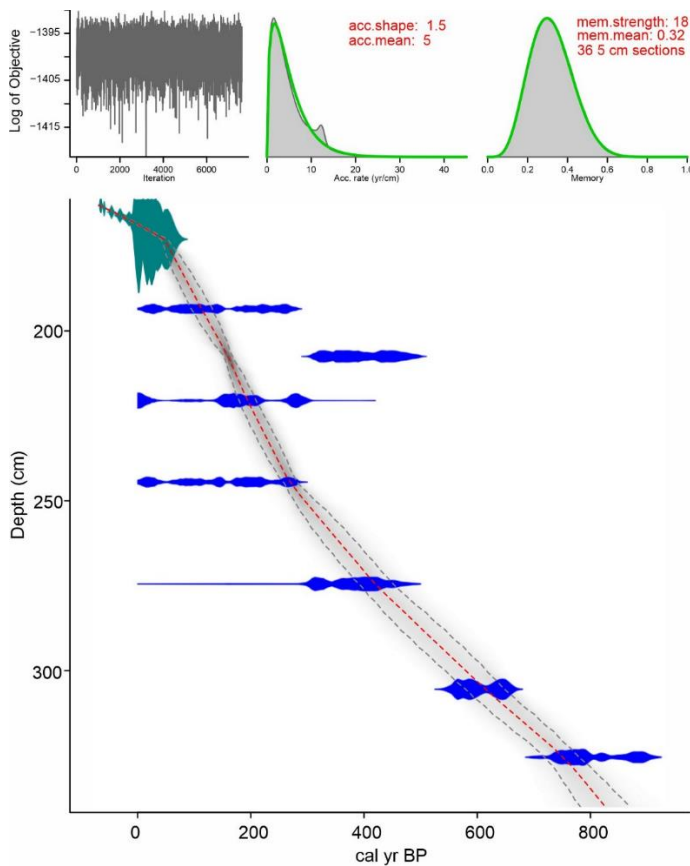
973 spore data to study fire events in the boreal forest of northern Europe. *The Holocene* 29(9),1480–
974 1490. <https://doi.org/10.1177/0959683619854524>
975
976 Stockmarr, J., 1972. Tablets with spores used in absolute pollen analysis. *Pollen and Spores* 13, 614–
977 621.
978
979 Svoboda, M., Janda, P., Báce, R., Shawn Fraver, S., Nagel, T.A., Jan Rejzek, J., Mikoláš, M., Douda, J.,
980 Boublík, K., Šamonil, P., Čada, V., Trotsiuk, V., Teodosiu, M., Bouriaud, O., Biriş, A.I., Sýkora, O., Uzel,
981 P., Zelenka, J., Sedlák, V., Lehejček, J., 2013. Landscape-level variability in historical disturbance in
982 primary *Picea abies* mountain forests of the Eastern Carpathians, Romania. *J Veg Sci* 25(2),386–401.
983 <https://doi.org/10.1111/jvs.12109>
984
985 Thom, D., Seidl, R., Steyrer, G., Krehan, H., Formayer, H., 2013. Slow and fast drivers of the natural
986 disturbance regime in Central European forest ecosystems. *For. Ecol. Manag.* 307, 293–302.
987 <https://doi.org/10.1016/j.foreco.2013.07.017>
988
989 Thom, D., Rammer, W., Seidl, R., 2017. Disturbances catalyze the adaptation of forest ecosystems to
990 changing climate conditions. *Global Change Biol.* 23,269–282. <https://doi.org/10.1111/gcb.13506>
991
992 Tolasz, R., Míková, T., Valeriánová, A., Voženílek, V., 2007. *Climate Atlas of Czechia*.
993 ČHMÚ/Palacký University, Prague/Olomouc.
994
995 Zatloukal, V., 1998. Historické a současné příčiny k rovcové kalamity v Národním parku Šumava. *Silva*
996 *Gabreta* 2, 327–357.
997
998 Whitlock, C., Larsen, C., 2001. Charcoal as a fire proxy, in: Smol, J.P., Birks, H.J.B., Last, W.M. (Eds.),
999 *Tracking Environmental Change Using Lake Sediments*. Springer, Dordrecht, 75–97.
1000 https://doi.org/10.1007/0-306-47668-1_5
1001
1002
1003
1004
1005
1006
1007

1008 **Figures and captions:**



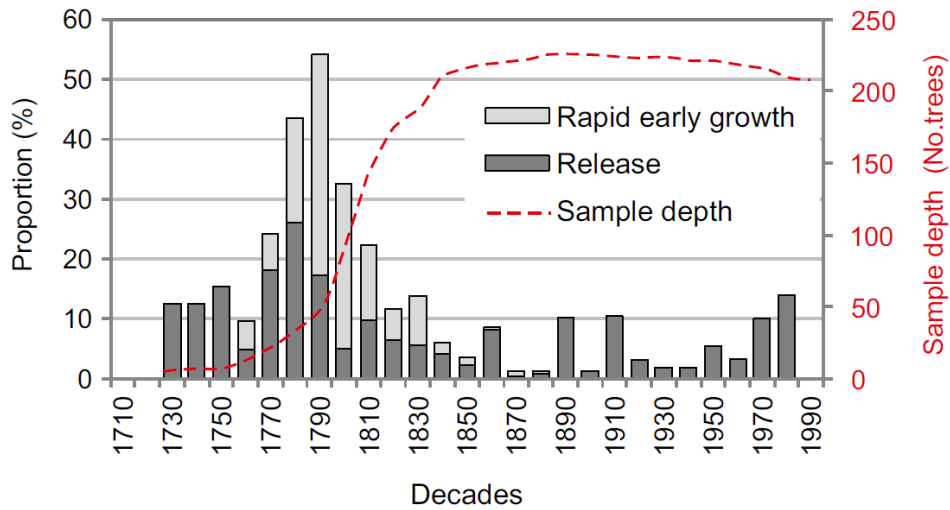
1009

1010 Figure 1. Research area in Bohemian/Bavarian forest is marked in the map on the right with red
1011 square and map in left shows the study area with coring site (star) and dendrochronological study
1012 plots (dots).
1013



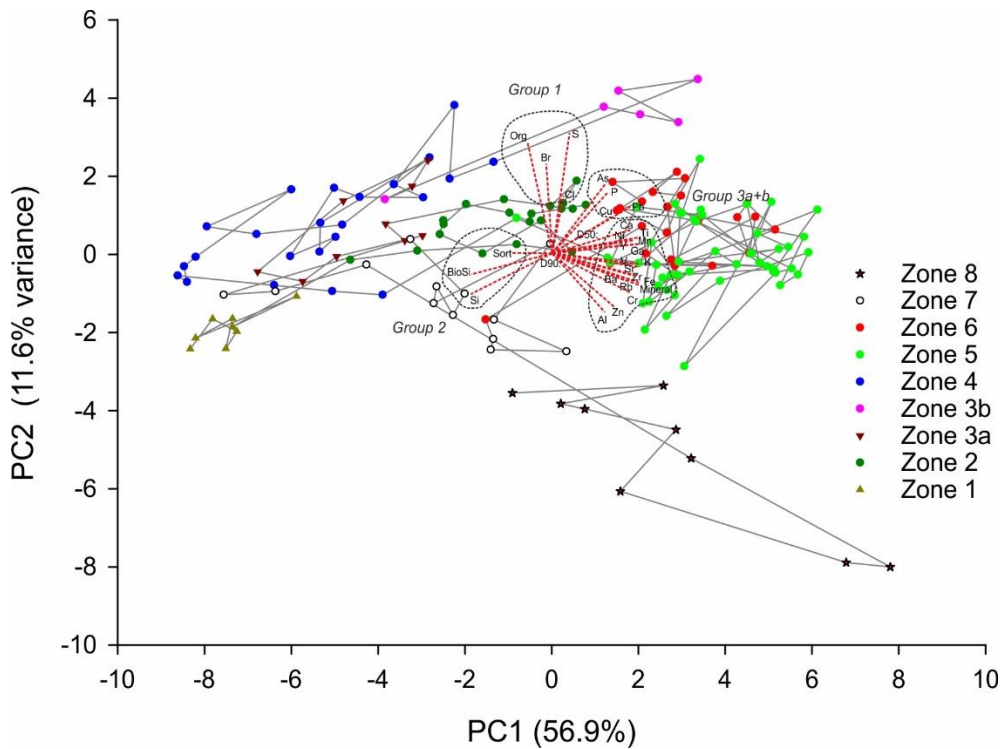
1014

1015 Figure 2. 'Bacon' age-depth model for the integrated Laka core based on seven radiocarbon ages and
1016 the ^{210}Pb and ^{137}Cs radionuclide dating series.



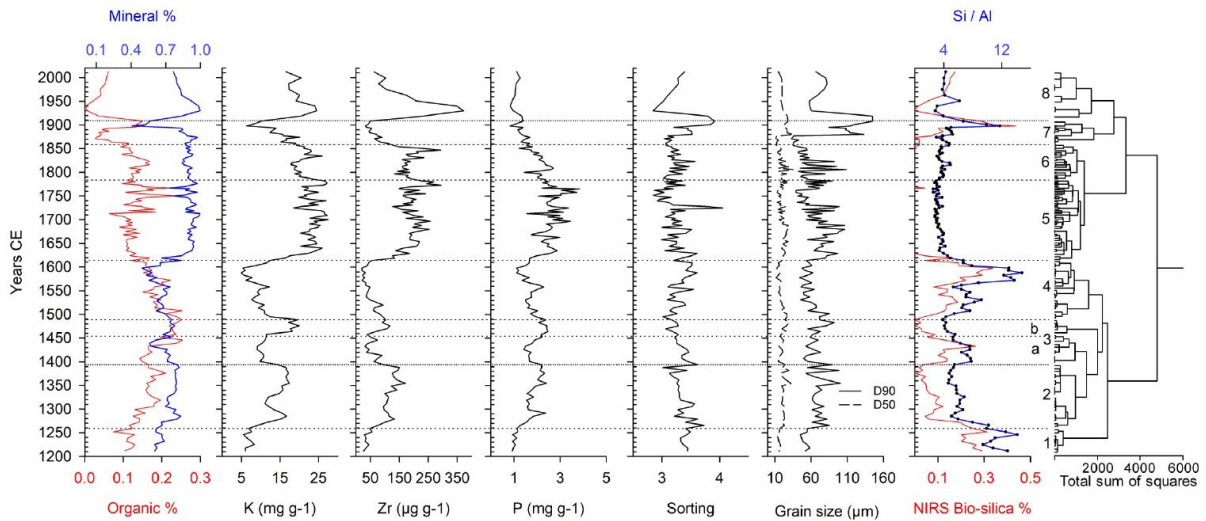
1017

1018 Figure 3. Tree-ring based disturbance history of the forest stand in the catchment of Laka, Šumava
 1019 NP, Czech Republic. Decadal resolved disturbance rate (columns) showing the proportion of affected
 1020 trees was compiled from 6 study plots with 224 trees located throughout the catchment. The trend
 1021 in number of available individual tree-ring series (tree age-structure) is shown with red dashed line.
 1022



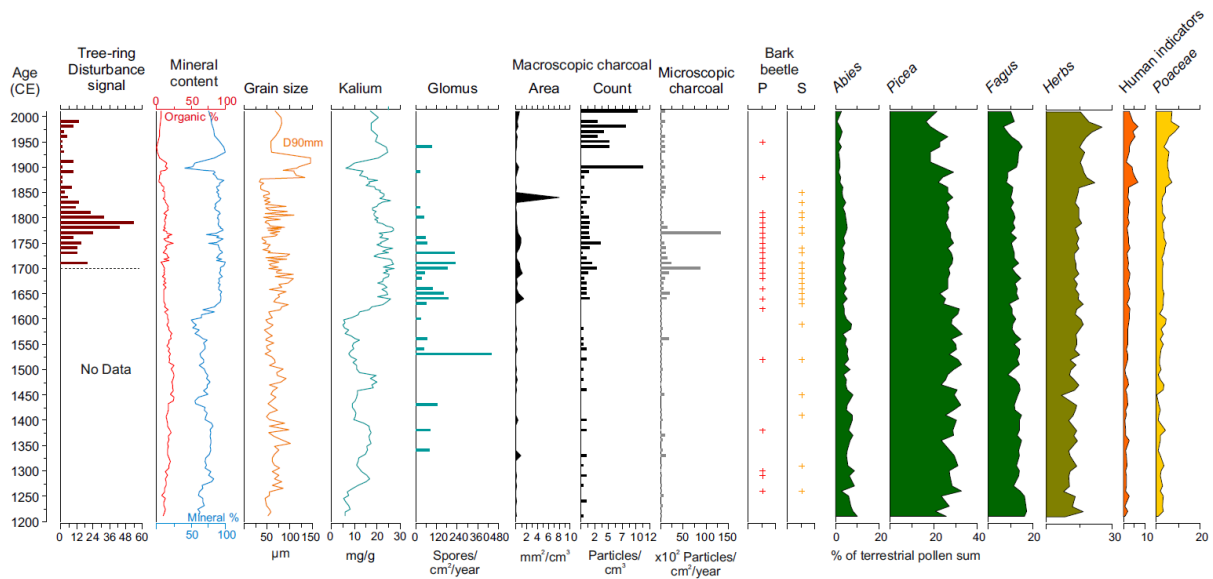
1023

1024 Figure 4. Biplot of Principal Component Analysis axes 1 and 2 calculating for geochemical, NIRS end
 1025 member components and grain size parameters (d90, d50 and sorting) showing three distinct
 1026 groupings of parameters. Sample PCA coordinates are colored by zones delimited using a
 1027 stratigraphical cluster analysis for all variables.



1028

1029 Figure 5. Physical properties for the Laka sediment profile plotted against the age-depth model (cal.
 1030 years CE) showing the relative proportions of NIRS-inferred mineral and organic content, element
 1031 concentrations (ED-XRF) for K, Zr and P, degree of sorting, d90 and d90 of the grain size distributions,
 1032 and NIRS inferred biogenic silica alongside the Si:Al element ratio. The dendrogram reports a
 1033 stratigraphical cluster analysis for all variables standardized to mean = 0 and ± 1 standard deviation,
 1034 which informed the zone boundaries (1-8).



1035

1036 Figure 6. Diagram showing tree-ring based disturbance signal in decadal resolution, mineral content
 1037 (%), grain size (μm) and Kalium (mg/g) as sedimentological proxies for erosion in the lake catchment
 1038 and palaeoecological proxies Glomus fungal spore influx, macroscopic charcoal concentrations
 1039 (particles cm^{-3}) and area measurements ($\text{mm}^2 \text{cm}^{-3}$), microscopic charcoal influx, presence of primary
 1040 (P) and secondary (S) bark beetles, pollen curves for main forest forming tree taxa *Abies*, *Picea* and
 1041 *Fagus*, sum of herbaceous pollen taxa sum of human indicator pollen taxa (*Cerealia* sp., *Secale*,
 1042 *Plantago* sp. *Rumex*) and *Poaceae* in 10 year temporal resolution.

1043

1044